MENU 2007
11th International Conference
on Meson-Nucleon Physics and
the Structure of the Nucleon
September10-14, 2007
IKP, Forschungzentrum Jülich, Germany

NEUTRON POLARISABILITIES FROM DEUTERON COMPTON SCATTERING IN χEFT

Harald W. Grießhammer
Center for Nuclear Studies, Department of Physics,
The George Washington University, Washington DC 20052, USA

Abstract

Chiral Effective Field Theory is for photon energies up to 200 MeV the tool to accurately determine the polarisabilities of the neutron from deuteron Compton scattering. A multipole analysis reveals that dispersive effects from an explicit $\Delta(1232)$ prove in particular indispensable to understand the data at 95 MeV measured at SAL. Simple power-counting arguments derived from nuclear phenomenology lead to the correct Thomson limit and gauge invariance. At next-to-leading order, the static scalar dipole polarisabilities are extracted as identical for proton and neutron within the error-bar of available data: $\overline{\alpha}^n = 11.6 \pm 1.5_{\text{stat}} \pm 0.6_{\text{Baldin}}, \overline{\beta}^n = 3.6 \mp 1.5_{\text{stat}} \pm 0.6_{\text{Baldin}}$ for the neutron, in units of 10^{-4} fm^3, compared to $\overline{\alpha}^p = 11.0 \pm 1.4_{\text{stat}} \pm 0.4_{\text{Baldin}}$, $\overline{\beta}^p = 2.8 \mp 1.4_{\text{stat}} \pm 0.4_{\text{Baldin}}$ for the proton in the same framework. New experiments e.g. at MAXlab (Lund) will improve the statistical error-bar.

1 The Problem with Neutron Polarisabilities

As the nucleon is not a point-like spin-$\frac{1}{2}$ target with an anomalous magnetic moment, the photon field displaces in low-energy Compton scattering $\gamma N \to \gamma N$ its charged constituents, inducing a non-vanishing multipole-moment. These long-known nucleon-structure effects are for static external fields parameterised by the electric polarisability $\overline{\alpha}$ and its magnetic counter-part $\overline{\beta}$. For the proton, the generally accepted static values are $\overline{\alpha}^p \approx 12 \times 10^{-4}$ fm^3, $\overline{\beta}^p \approx 2 \times 10^{-4}$ fm^3, with error-bars of about 1. [1]

Does the neutron react similarly under deformations, $\overline{\alpha}^p \approx \overline{\alpha}^n$, $\overline{\beta}^p \approx \overline{\beta}^n$? Different types of experiments report a range of values $\overline{\alpha}^n \in [-4; 19]$: Coulomb scattering of neutrons off lead, and deuteron Compton-scattering $\gamma d \to \gamma d$ with and without breakup, see e.g. [1] for a list. The latter should be

[1] It is customary to measure the scalar dipole-polarisabilities in 10^{-4} fm^3, so that the units are dropped in the following. Notice that the nucleon is quite stiff.

a clean way to extract the iso-scalar polarisabilities $\overline{\alpha}^s := \frac{1}{2}(\overline{\alpha}^p + \overline{\alpha}^n)$ and $\overline{\beta}^s$ in analogy to determinations of the proton polarisabilities. Experiments were performed in Urbana at $\omega = 49$ and 69 MeV, in Saskatoon (SAL) at 94 MeV, and in Lund (MAXlab) at 55 and 66 MeV. While all low-energy extractions are consistent with small iso-vectorial polarisabilities, the SAL data lead to conflicting analyses: The original publication [2] gave $\overline{\alpha}^s = 8.8 \pm 1.0$, using the Baldin sum-rule for the static nucleon polarisabilities. Without it, Levchuk and L'vov obtained $\overline{\alpha}^s = 11 \pm 2$, $\overline{\beta}^s = 7 \pm 2$ [3]; and Beane et al. found recently from all data $\overline{\alpha}^s = 13 \pm 4$, $\overline{\beta}^s = -2 \pm 3$ [4]. The extraction being very sensitive to the polarisabilities, this seems discouraging news.

These notes outline the resolution of the puzzle and report on a new high-accuracy determination of the nucleon polarisabilities from all Compton scattering data. There are two main ingredients: a better understanding of dispersive effects in the polarisabilities themselves as discussed in Sect. 2; and a model-independent determination of meson-exchange current effects with an error-estimate, Sect. 3. As customary in proceedings, I apologise for my biased view and refer to [1] at least for a better list of references.

2 Dynamical Polarisabilities

The nucleon-structure effects encoded by the polarisabilities are conveniently parameterised starting from the most general interaction between a nucleon N with spin $\vec{\sigma}/2$ and an electro-magnetic field of fixed, non-zero energy ω:

$$\begin{aligned} \mathcal{L}_{\text{pol}} = 2\pi N^\dagger \big[&\alpha_{E1}(\omega)\vec{E}^2 + \beta_{M1}(\omega)\vec{B}^2 + \gamma_{E1E1}(\omega)\vec{\sigma}\cdot(\vec{E}\times\dot{\vec{E}}) \\ &+ \gamma_{M1M1}(\omega)\vec{\sigma}\cdot(\vec{B}\times\dot{\vec{B}}) - 2\gamma_{M1E2}(\omega)\sigma_i B_j E_{ij} + 2\gamma_{E1M2}(\omega)\sigma_i E_j B_{ij} + \dots \big] N \end{aligned} \tag{1}$$

Here, the electric or magnetic ($X, Y = E, M$) photon undergoes a transition $Xl \to Yl'$ of definite multipolarity $l, l' = l \pm \{0, 1\}$; $T_{ij} := \frac{1}{2}(\partial_i T_j + \partial_j T_i)$. Its coefficients are the *energy-dependent* or *dynamical polarisabilities* of the nucleon [5]. Most prominently, there are six dipole-polarisabilities. The two spin-independent ones parameterise electric and magnetic dipole-transitions, $\alpha_{E1}(\omega)$ and $\beta_{M1}(\omega)$. Particularly interesting are the four spin-polarisabilities $\gamma_{E1E1}(\omega)$, $\gamma_{M1M1}(\omega)$, $\gamma_{E1M2}(\omega)$, $\gamma_{M1E2}(\omega)$ as they parameterise the response of the nucleon-*spin* to the photon field. Contributions from higher ones like quadrupole polarisabilities are negligible in today's experiments.

Polarisabilities measure the global stiffness of the nucleon's internal degrees of freedom against displacement in an electric or magnetic field of definite multipolarity and non-vanishing frequency ω and are identified *at fixed* *energy* only by their different angular dependence. Nucleon Compton scattering provides thus a wealth of information about the internal structure of the nucleon. In contradistinction to most other electro-magnetic processes, the nucleon-structure effects in Compton scattering were however previously not analysed in terms of a multipole-expansion at fixed energies. Instead, one focused on the static electric and magnetic polarisabilities $\overline{\alpha} := \alpha_{E1}(\omega = 0)$ and $\overline{\beta} := \beta_{M1}(\omega = 0)$, which are often called "the polarisabilities". While quite different frameworks could provide a consistent picture for them, the underlying mechanisms are only properly revealed by the energy-dependence.

Clearly, the complete set of dynamical polarisabilities does – like in all multipole-decompositions – not contain more or less information about the temporal response of the nucleonic degrees of freedom than the Compton amplitudes. But the information is better accessible and easier to interpret, as each mechanism leaves a characteristic signature in a particular channel.

To investigate them in a model-independent framework, we employ the unique low-energy theory of QCD, namely Chiral Effective Field Theory χEFT. It contains only those low-energy degrees of freedom which are observed at the typical energy of the process, interacting in all ways allowed by the underlying symmetries of QCD. A momentum expansion of all forces allows for model-independent results of finite, systematically improvable accuracy and thus for an estimate of the theoretical uncertainties encountered by neglecting higher-order contributions. The resulting contributions at leading order (LO) are listed in Fig. 1 and easily motivated [5]:

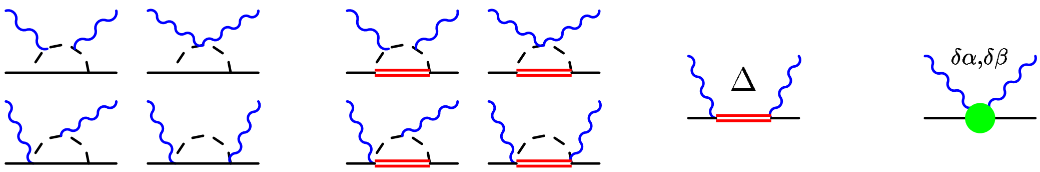

Figure 1: The LO contributions to the nucleon polarisabilities. Left to right: pion cloud around the nucleon and Δ; Δ excitations; short-distance effects. Permutations and crossed diagrams not shown. From Ref. [5].

(1) Photons couple to the pions around the nucleon and around the Δ, signalled by a characteristic cusp at the one-pion production threshold.

(2) It is well-known that the Δ(1232) as the lowest nuclear resonance leads by the strong $\gamma N\Delta$ $M1$-transition to a para-magnetic contribution to the static magnetic dipole-polarisability $\overline{\beta}_{\Delta} = +[7\dots13]$ and a characteristic resonance-shape, cf. the Lorentz-Drude model of classical electrodynamics.

(3) As the observed static value $\overline{\beta}^p \approx 2$ is smaller by a factor of 5 than the

Δ contribution, a strong dia-magnetic component must exist. The resultant fine-tuning at zero photon-energy is unlikely to hold once the evolution with the photon energy is considered: If dia- and para-magnetism are of different origin, they involve different scales and hence different energy-dependences. We sub-sume this short-distance Physics which is at this order not generated by the pion or Δ into two *energy-independent* low-energy coefficients $\delta\alpha$, $\delta\beta$.

The cornucopia of Compton data on the proton below 200 MeV determines these to be indeed anomalously large, $\delta\alpha = -5.9 \pm 1.4$, $\delta\beta = -10.7 \pm 1.2$, justifying their inclusion at leading order. As expected, $\delta\beta$ is dia-magnetic. The resulting static proton polarisabilities

$$\overline{\alpha}^p = 11.0 \pm 1.4_{\text{stat}} \pm 0.4_{\text{Baldin}} \quad , \quad \overline{\beta}^p = 2.8 \mp 1.4_{\text{stat}} \pm 0.4_{\text{Baldin}} \tag{2}$$

compare both in magnitude and uncertainty favourably with other state-of-the-art results [5]. Higher-order corrections contribute an error of about ± 1 not displayed here as the statistics dominates the total error.

With the parameters now fixed, the energy-dependence of all polarisabilities is fixed. χEFT predicts them at LO to be identical for the proton and neutron. We will confirm this in Sect. 3. The dipole-polarisabilities show the expected behaviour. No low-energy degrees of freedom inside the nucleon are missing. Dispersion is large for $\omega \in [80; 200]$ MeV where most experiments to determine polarisabilities are performed. Most notably even well below the pion-production threshold is the strong energy-dependence induced into $\beta_{M1}(\omega)$ and all polarisabilities containing an $M1$ photon by the unique signature of the Δ-resonance: Truncating the Taylor-expansion at order ω^2 under-estimates $\beta_{M1}(\omega = 95\text{ MeV})$-$\overline{\beta} \approx 1.7$ [3], while the multipole-analysis gives ≈ 4 (Fig. 2). The traditional approximation of $\beta_{M1}(\omega)$ as "static-plus-small-slope", $\overline{\beta} + \omega^2 \overline{\beta}_\nu$, is inadequate. Not surprisingly, this contribution is most pronounced at large momentum-transfers, i.e. backward angles, and thus is the major source of confusion in deuteron Compton scattering, as Fig. 5 will show. Figure 2 reveals the good agreement between the measured value of $\overline{\beta}^p$ and the prediction in χEFT without explicit Δ as accidental: The pion is not dispersive enough to explain the energy-dependence of β_{M1}.

That the two short-distance parameters $\delta\alpha$, $\delta\beta$ suffice to describe the data up to $\omega \approx 200$ MeV [5] leads to three constraints on their explanation:

(1) Like $\delta\alpha$, $\delta\beta$, the effect must be ω-independent over a wide range.

(2) Albeit it must lead to the values for $\delta\alpha$, $\delta\beta$ predicted in χEFT, it must be absent at least in the pure spin-polarisabilities γ_{E1E1}, γ_{M1M1}.

(3) Its prediction for the proton and neutron must be similar because iso-vectorial effects are small and energy-independent [5, 6].

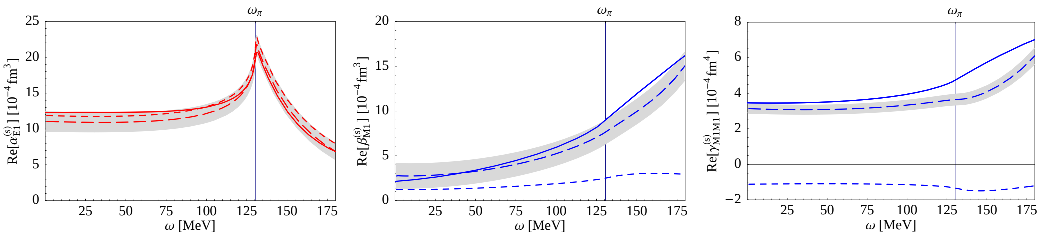

Figure 2: Spin-independent (left, right) and example of spin-dependent (right) dipole-polarisabilities, predicted by Dispersion Theory (solid) and χEFT with (dashed; band: fit-errors) and without (dotted) explicit Δ. ω_π: one-pion production threshold. From Ref. [5].

3 Embedding the Nucleon in the Deuteron

Since free neutrons can often not be used in experiments, their properties are usually extracted from data taken on few-nucleon systems by dis-entangling nuclear-binding effects. χEFT allows to subtract two-body contributions from meson-exchange currents and wave-function dependence from data with minimal theoretical prejudice and an estimate of the theoretical uncertainties.

A consistent description must also give the correct Thomson limit, i.e. the exact low-energy theorem which is a consequence of gauge invariance [7, 8]. Its verification is straight-forward in the 1-nucleon sector, where the ampli-

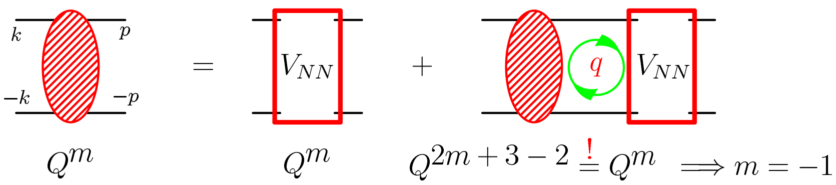

Figure 3: On the consistency of NN power-counting in χEFT. From Ref. [9].

tude is perturbative. In contradistinction, the two-nucleon amplitude must be non-perturbative to accommodate the shallow bound-state: All terms in the LO Lippmann-Schwinger equation of NN-scattering, Fig. 3, including the potential, must be of the same order when all nucleons are close to their non-relativistic mass-shell. Otherwise, one of them could be treated as perturbation of the others and a low-lying bound-state would be absent. Picking the nucleon-pole in the energy-integration $E \sim \frac{\vec{k}^2}{2M}$ leads therefore to the consistency condition that the NN-scattering amplitude T_{NN} must be of order Q^{-1}, irrespective of the potential used. Q is a typical low-momentum scale of the process under consideration, e.g. the inverse S-wave scattering length. It does therefore not suffice to determine the relative strength of forces and potentials in χEFT just by counting the number of momenta. This has long been recognised in "pion-less" EFT, but is only an emerging communal wisdom in the chiral version [9–11].

In deuteron Compton scattering, this mandates inclusion of T_{NN} for all graphs in which both nucleons propagate close to their mass-shell between photon absorption and emission, i.e. in which the photon energy $\omega \lesssim 50$ MeV does not suffice to knock a nucleon far off its mass-shell [1, 9]. Figure 4 lists the contributions to Compton scattering off the deuteron to next-to-leading order NLO in χEFT. At higher photon energies $\omega \gtrsim 60$ MeV, on can show that the nucleon is kicked far off its mass-shell, $E \sim |\vec{k}|$, and the amplitude becomes perturbative. This is intuitively clear, as the nucleon has only a very short time ($\sim 1/\omega$) to scatter with its partner before the second photon has to be radiated to restore the coherent final state. The diagrams which contain T_{NN} in Fig. 4 are therefore less important for larger ω, together with some of the other diagrams. Indeed, the nucleon propagator scales then as $1/Q \sim 1/\omega$ and thus becomes static, with each re-scattering process in T_{NN} suppressed by an additional power of Q.

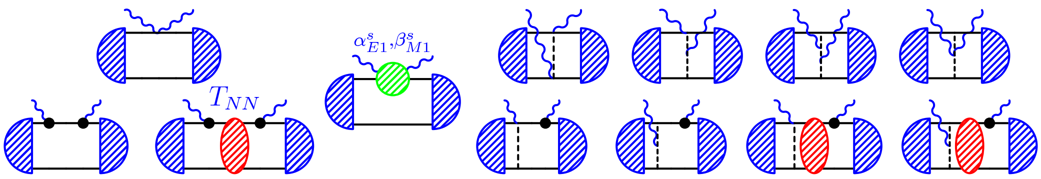

Figure 4: Deuteron Compton scattering in χEFT to NLO. Left: one-body part (dot: electric/magnetic coupling; blob: nucleon polarisabilities of Fig. 1). Right: two-body part (pion-exchange currents). Permutations and crossed graphs not shown. From Ref. [1].

We implemented rescattering by the Green's function method described in [1, 3, 12]. The calculation is parameter-free when the short-distance coefficients $\delta\alpha$, $\delta\beta$ are taken over from the proton – as justified by the χEFT prediction that iso-vectorial contributions are suppressed by one order. The nucleon- and nuclear-structure contributions separate at this (and the next) order. While the two-nucleon piece does not contain the $\Delta(1232)$-resonance in the intermediate state at this order as the deuteron is an iso-scalar target, this does not hold for the polarisabilities, as seen in Sect 2. Figure 5 also shows that the strong energy-dependence from the Δ is indeed pivotal to reproduce both shape and normalisation of the 94 MeV data in particular at back-angles without significantly changing the static polarisabilities, but is negligible at lower energies. Thus, we argue that the discrepancy between the SAL data and experiments at lower energies is resolved [1, 6].

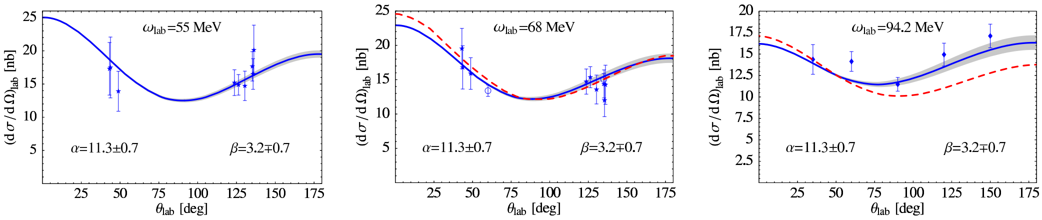

Figure 5: Examples for the 1-parameter fit result using the Baldin sum rule (solid, with stat. uncertainty), compared to χEFT without explicit $\Delta(1232)$ ($\mathcal{O}(p^3)$, dashed). From Ref. [1].

The power-counting at the heart of χEFT implies several cross-checks: First, it must automatically reproduce the Thomson limit as an exact LO result, with all corrections cancelling order by order as $\omega \to 0$ [7]. Fortunately, Arenhövel showed long before χEFT was formulated that it is indeed exactly recovered from the diagrams which χEFT classifies as LO at low energies, and that all diagrams which couple photons to meson-exchange currents sum up to zero at zero energy [8]. The numerical calculation confirms this [1].

Secondly, χEFT demotes at higher photon energies all graphs with T_{NN} in the intermediate state to higher orders. The difference to the previous χEFT calculations [4, 6] which were tailored to high photon energies should therefore decrease with increasing ω. This is indeed found, see Fig. 6.

Another consequence is a substantially reduced dependence on the deuteron wave-function, see Fig. 7. With the long-range part fixed by the deuteron binding energy and one-pion exchange, different wave-functions and potentials correspond to different assumptions about the short-distance dynamics of NN-scattering. Different answers would hence indict model-dependence,

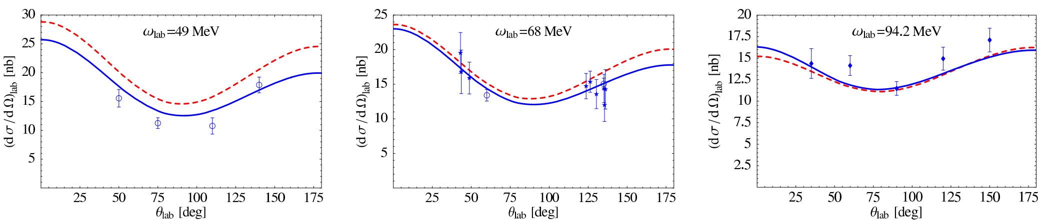

Figure 6: Examples of prediction using proton polarisabilities with (solid) and without (dashed) NN-rescattering in intermediate states. From Ref. [1].

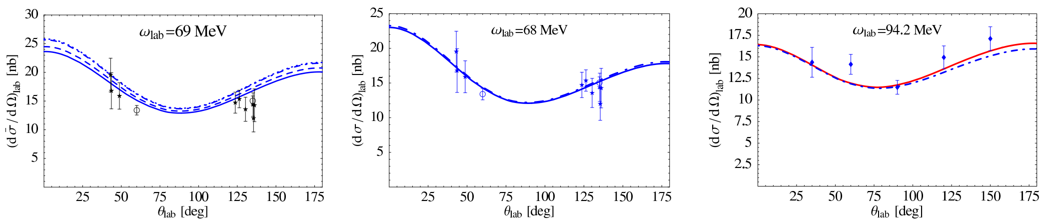

Figure 7: Examples of dependence on higher-order effects, with iso-scalar polarisabilities at proton values. Left (without T_{NN}) and centre (with T_{NN}): different deuteron wave-functions (solid: NNLO χEFT; dot-dashed: AV18; dashed: CD-Bonn; dotted: Nijmegen 93). Right: Dependence on the NN-potential for T_{NN} (solid: LO χEFT; dot-dashed: AV18). From Ref. [1].

i.e. sensitivity to details of Physics at scales where a description in terms of the low-energy degrees of freedom breaks down. In the model-*independent* approach of χEFT, answers from different potentials and wave-functions agree within the theoretical accuracy, i.e. serve to estimate higher-order contributions. While the Thomson limit is universal for $\omega \to 0$ [7, 8], the dependence on the deuteron wave-function used is now also at higher energies virtually eliminated compared to previous approaches [4, 6].

Figure 7 shows that the result is also quite insensitive to the potential from which T_{NN} is found. The maximal difference is smaller than 3% between constructing it from AV18 and a one-pion exchange with a crude parameterisation of short-distance effects as two point-like, momentum-independent contact operators. In χEFT, these differences come from NN interactions which are suppressed by $Q^2 \approx (1/7)^2$, in line with the spread found.

Finally, we test whether the neutron and proton polarisabilities are indeed similar by fitting the two short-distance parameters $\delta\alpha$, $\delta\beta$ to all deuteron Compton scattering data below 100 MeV [1]. The iso-scalar Baldin sum rule $\overline{\alpha}^s+\overline{\beta}^s = 14.5\pm0.6$ is in excellent agreement with our 2-parameter fit, serving in the next step as input to model-independently determine the iso-scalar, spin-independent dipole polarisabilities of the nucleon at zero energy:

$$\overline{\alpha}^s = 11.3 \pm 0.7_{\text{stat}} \pm 0.6_{\text{Baldin}} \pm 1_{\text{th}} \;,\; \overline{\beta}^s = 3.2 \mp 0.7_{\text{stat}} \pm 0.6_{\text{Baldin}} \pm 1_{\text{th}} \quad (3)$$

We estimate the theoretical error to be ±1 from typical higher-order contributions in the one- and two-nucleon sector. Comparing this with our analysis (2) of all proton Compton data below 170 MeV by the same method, we conclude that the proton and neutron polarisabilities are to this leading order identical within (predominantly statistical) errors and confirm the χEFT prediction. In particular, the proton and neutron show only a small but very similar deformation when put between the poles of a magnet: $\overline{\beta}^p \approx \overline{\beta}^n \approx 3$.

4 Concluding Questions

Dynamical polarisabilities test the global response of the nucleon to the electric and magnetic fields of a real photon with non-zero energy and definite multipolarity. They answer the question which internal degrees of freedom govern the structure of the nucleon at low energies and are defined by a multipole-expansion of the Compton amplitudes. While they do not contain more or less information than the corresponding Compton scattering amplitudes, the facts are more readily accessible and easier to interpret. Dispersive effects in particular from the $\Delta(1232)$ are necessary to accurately extract the static polarisabilities of the nucleon from all data. Future work includes:

(i) The non-zero width of the Δ and higher-order effects from the pion-cloud become crucial in the resonance region.

(ii) A multipole-analysis of Compton scattering at fixed energies from doubly-polarised, high-accuracy experiments provides a new avenue to extract the energy-dependence of the six dipole-polarisabilities per nucleon, both spin-independent and spin-dependent [5]. This will in particular further our knowledge on the spin-polarisabilities which characterise the spin-structure of the nucleon. A concerted effort of planned and approved experiments at $\omega \lesssim 300$ MeV is under way: polarised photons on polarised protons, deuterons and ^{3}He at TUNL/HIγS; tagged protons at S-DALINAC; polarised photons on polarised protons at MAMI. An unpolarised, running experiment on the deuteron at MAXlab covers a wide range of energies and angles. With at present only 29 (un-polarised) points for the deuteron in a small energy range of $\omega \in [49; 94]$ MeV and error-bars on the order of 15%, these high-quality data will provide better information on the neutron polarisabilities and allow one to zoom in on the proton-neutron differences.

(iii) Choudhury et al. found that Compton scattering on ^{3}He also shows high sensitivity to the neutron polarisabilities [13]. In a coordinated effort, we now investigate which observables in proton, deuteron and ^{3}He Compton scattering are most sensitive to combinations of polarisabilities in χEFT. Of particular interest are polarisation asymmetries because of their sensitivity to the experimentally practically undetermined dipole spin-polarisabilities.

Enlightening insight into the electro-magnetic structure of the nucleon has already been gained from combining Compton scattering off nucleons and few-nucleon systems with χEFT and the (energy-dependent) dynamical polarisabilities; and a host of activities should add to it in the coming years.

Acknowledgements

I am grateful for financial support by the National Science Foundation (CAREER grant PHY-0645498), US Department of Energy (DE-FG02-95ER-40907) and Deutsche Forschungsgemeinschaft (GR1887/3-1). Foremost, I thank my collaborators – R.P. Hildebrandt, T.R. Hemmert, B. Pasquini and D.R. Phillips – for a lot of fun!

References

[1] R.P. Hildebrandt et al., [nucl-th/0512063], submitted to Phys. Rev. C; R.P. Hildebrandt, PhD thesis TU München Dec. 2005 [nucl-th/0512064].

[2] D.L. Hornidge et al., Phys. Rev. Lett. **84**, 2334 (2000).

[3] M.I. Levchuk and A.I. L'vov, Nucl. Phys. A**674**, 449 (2000).

[4] S.R. Beane, et al., Nucl. Phys. A**656**, 367 (1999); S.R. Beane et al., Phys. Lett. B**567**, 200 (2003); erratum ibid. B**607**, 320 (2005); Nucl. Phys. A**747**, 311 (2005).

[5] H. W. Grießhammer and T. R. Hemmert, Phys. Rev. C**65**, 045207 (2004); R. P. Hildebrandt et al., Eur. Phys. J. A**20**, 293 (2004); H. W. Grießhammer, Prog. Part. Nucl. Phys. **55**, 215 (2005).

[6] R.P. Hildebrandt et al., Nucl. Phys. A**748**, 573 (2005).

[7] J.L. Friar, Ann. of Phys. **95**, 170 (1975).

[8] H. Arenhövel, Z. Phys. A**297**, 129 (1980); M. Weyrauch and H. Arenhövel, Nucl. Phys. A**408**, 425 (1983).

[9] H.W. Grießhammer, forthcoming.

[10] A. Nogga et al., Phys. Rev. C**72**, 054006 (2005); M.C. Birse, Phys. Rev. C**74**, 014003 (2006) and **76**, 034002 (2007).

[11] H. W. Grießhammer, Nucl. Phys. A**760** 110 (2007).

[12] J.J. Karakowski and G.A. Miller, Phys. Rev. C**60**, 014001 (1999); J.J. Karakowski, Ph.D. thesis U. of Washington 1999 [nucl-th/9901011].

[13] D. Choudhury et al., Phys. Rev. Lett. **98**, 232303 (2007).